International Journal of Hydrogen Energy 78 (2024) 793–804

Contents lists available at ScienceDirect

International Journal of Hydrogen Energy

journal homepage: www.elsevier.com/locate/he

Structure modification of magnesium hydride for solid hydrogen storage

Haoliang Hong, Hangzuo Guo, Zhanfeng Cui, Anthony Ball, Binjian Nie *

Department of Engineering Science, University of Oxford, Oxford, OX1 3PJ, United Kingdom

ARTICLE INFO

Handling Editor: Umit Koylu

Keywords:
Magnesium hydride
Porous structure
Hydrogen storage

ABSTRACT

Hydrogen has received widespread attention as a clean future energy source. However, the key challenge to enable hydrogen as an energy vector is its storage. When comparing the various hydrogen storage methodologies, solid hydrogen storage using metal hydrides is quite attractive due to its high Volumatic energy density and high safety. In this review, we comprehensively discuss the critical importance of structural optimization, such as increasing porosity, for magnesium-based hydrogen storage materials. This aspect has been inadequately addressed and incompletely covered in previous works. Specifically, we present the hydrogen storage mechanisms by solid materials, particularly metal materials, along with their kinetic and thermodynamic principles. Additionally, synthesis methods of these materials using ball milling, thin film deposition, and direct current plasma technology are systematically classified and described. Performance improvements of Mg-based alloys or composites through catalysis, alloying and nanosizing were screened and concluded. Finally, porous-structure based improvements for Mg-based materials are emphasized, including Mg porous films, Mg metal-organic framework sand Mg-based nanoconfined materials. This study concludes that a bio-inspired technique for creating porous magnesium skeletons shows significant potential and advantages. Additionally, a casting method incorporating ultrasound is identified as an efficient solution for large-scale production. These technological innovations can replace expensive rare earth elements while achieving similar effects.

1. Introduction

The energy demand of various industry sectors is anticipated to continuously expand globally, such as the construction and cement industries [1–3], the information technology and artificial intelligence fields [4], the healthcare industry [5], as well as fuel and engines [6,7]. Naturally, hydrogen, hailed for its cleanliness and renewability with a multitude of alternative raw sources (i.e., methane [8], ammonia [9] or microalgae [10]), as well as storage configurations [11] and applications [12], is heralded by governments as the vanguard of future energy which is anticipated to claim an absolute majority in total energy utilization by 2050 [13,14]. Hydrogen boasts commendable attributes, for instance, minimal weight with low density (0.089 g/L at STP) and impressive energy density (119.96 MJ/kg for lower heating value). However, gaseous hydrogen reveals a significantly heightened degree of instability [15]. Factors about hydrogen including a lower ignition temperature (574 °C, compared to natural gas at 650 °C), a broader flammability range (4–75 vol% in air, versus 5–15 vol% for natural gas), and a faster burning velocity (2.65–3.25 m/s, as opposed to 0.38 m/s for natural gas) contribute to substantial safety limitations and challenges in the storage, transportation, and utilization of hydrogen [15–17].

Within the spectrum of processes governing hydrogen logistics, stockpiling, and application, the paramount significance lies in the domain of hydrogen storage technology. Several methods for hydrogen storage have been developed. Currently, two predominant categorizations exist: the first delineates based on hydrogen storage states (i.e., solid, liquid, and gaseous storage methods) [18,19], and the second divides storage mechanisms into physical storage and chemical storage (also known as material-based storage) [20,21]. Fig. 1 [22] shows a comprehensive array of hydrogen storage mechanisms, with each subcategorized method distinctly labelled according to its prevailing state during the storage phase. In physical hydrogen storage, hydrogen can be formed into liquid or gaseous states by cooling, compression, or a combination of both [23]. Compressed gaseous hydrogen is generally conserved by means of vessel, geological storage, or other underground technologies [24]. Chemical storage presents numerous advantages and holds significant development potential over physical methods, particularly in terms of safety, stability, and the diversity of available methodologies [25]. Multi-microporous materials for adsorption can generally be categorized as crystalline or amorphous, and both

* Corresponding author.
E-mail address: binjian.nie@eng.ox.ac.uk (B. Nie).

https://doi.org/10.1016/j.ijhydene.2024.06.327
Received 3 May 2024; Received in revised form 21 June 2024; Accepted 24 June 2024
Available online 1 July 2024

categories can be subdivided into organic and inorganic materials [26–30]. Adsorption including particulate mass transfer utilizing metals hydrides (i.e., single or complex metal hydrides [31–35], metallic (interstitial) hydrides [36,37]) or chemical hydrides (e.g., boron compounds [38], ammonia [39], liquid organic hydrides (LOH) [40,41]), is another important research direction, especially metal compounds with their original structure [42], high heat recovery potential [43] and applicability to small and medium-sized applications [44,45]. Remarkably, in addition to the conventional solid-liquid-gas state, Lamb and Webb [46] has reviewed slush-state hydrogen storage technologies, a way of entrapping solid components in fluid, which shows advantages in terms of manoeuvrability, amount of storage and safety, for example, the oxidation phenomenon is dramatically reduced in magnesium hydride (MgH_2) slush even in the presence of air.

By conducting recent reviews in solid hydrogen storage, it's shown that most existing review papers centre their attention on summarizing metal hydrides, with an emphasize on complex metal hydrides, including lithium aluminium hydride [47,48] or sodium borohydride [49,50]. The remaining work concentrates on other storage materials including porous silicon [51], metal-organic frameworks (MOFs) [52], or porous carbon materials [53]. When narrowing to Mg-based materials, the recent reviews are presented as follow. Li et al. [54] started from the fundamental logic of Mg-based hydrogen storage, the thermodynamics and kinetics of hydrogen charge and discharge, and then highlighted such models as classical kinetics and quantum mechanics. The performance improvement methods including nanosizing, alloying, and adding rare-earth elements were reported as well. Similarly, Shang et al. [55], analysed hydrogen storage thermodynamics and kinetics to comparatively assess MgH_2 preparation methods over the past three decades, including ball milling, thin film and plasma technology. Yang et al. [56] summarized the influence of catalysts on MgH_2. It was shown that transition metals and rare-earth metals have the most remarkable contribution to the Mg/MgH_2 system, and ultrafine nanostructures. Ali and Ismail [57] summarized the fusion of MgH_2 and $NaAlH_4$ by ball milling to form a Mg–Na–Al system, which reduces the hydrogen desorption temperature, extends the cycle life and strengthens the kinetic properties. Ding et al. [58] and Ren et al. [59] had a particular emphasis on the impact of nanostructures materials, they concluded that the high cost of nanomaterials and the limited cycling stability block them toward large-scale applications.

2. Scope

The primary focus of this review scrutinizes solid-state and Mg-based hydrogen storage materials from an engineering application perspective, instead of a mere examination of materials. The significance and objectives of this work can be summarized as follows.

- To review hydrogen storage technologies in various states to elucidate the potential of solid-state materials in large-scale applications.
- To provide a comprehensive update on the latest research in Mg-based hydrogen storage materials with porous structures.
- To summarize and outlook the challenges and future development on performance improvement of Mg-based hydrogen storage materials with porous structure modification.

This paper works on the rationale behind the deliberate preference for solid-state materials over liquid, gaseous, and slush alternatives firstly. It will then intricately depict and compare various solid hydrogen storage materials to identify the great potential of Mg based materials. Finally, outlook and recommendations to facilitate porous-structured Mg-based materials are presented.

3. Solid hydrogen storage materials

Challenges associated with high pressures and low temperatures in compressed or cryogenic hydrogen storage can be addressed by solid-state materials which offer promising alternatives through physical or chemical hydrogen bonding. Table 1 selects a few representative hydrogen storage technologies.

Compared to compressed or cryogenic hydrogen storage, Solid-state hydrogen storage materials present advantages such as high storage density and superior safety. Koylu and Vudumu [68] utilized models and computational tools to analyse the dispersion and flammability of hydrogen gas released from a common storage tank into the air under various conditions. Their findings demonstrated that, compared to conventional fuel leaks, hydrogen leaks pose a relatively lower hazard. However, hydrogen stored in solid-state hydrogen storage systems even does not exist in its flammable elemental form, thus inherently reducing the likelihood of safety incidents from the outset. Various types of solid-state hydrogen storage materials have been approached include metal hydrides, carbon materials, metal-organic framework materials, covalent organic framework materials, two-dimensional transition metal carbide and carbon nitride materials (MXenes).

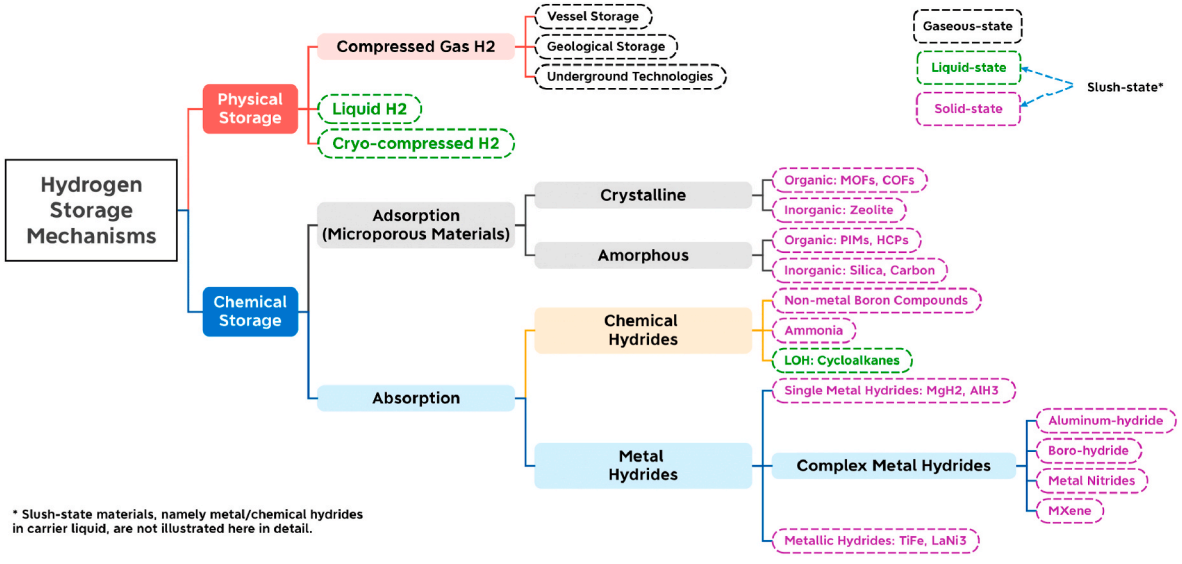

Fig. 1. Hydrogen storage methods catalogized by mechanisms.

Table 1
Overview of represented hydrogen storage methods.

Status	Mechanism	Gravimetric Capacity (wt. %)	Volumetric Energy Density (MJ/L)	Temperature (K)	Pressure (bar)	Comments	Ref.
Gas	Compressed	5.2	3.9[b]	293[a]	700	Type IV	[60]
Gas	Compressed	5.7	4.9	293	700	Existing Industrial Norms	[61]
Gas	Compressed	6.5	6.1	293	700	Compressed automotive hydrogen storage system	[62]
Liquid	Cryo-compressed	5.8	6.0[b]	~60	276	Cons: Evaporation	[60]
Liquid	Cryo-compressed	7.0	5.7[b]	60–100	350	Automotive cryo-compressed hydrogen vessels	[63]
Liquid	Cryogenic	7.5	6.4	20	Ambient	Desired Ultimate for Spherical Tanks	[64]
Liquid	LOHC	7.3	8.4[b]	293	Ambient	Naphthenic	[65]
Solid	Metal hydrides	7.3[b]	8.5	200–600	20	Li–Al Hydride for Mobile Fuel Cell Applications	[66]
Solid	MOF	9.9	7.3[b]	77	100	Porous MOF-based Material MFU-4l-Li	[67]

[a] 293 K normally represents room temperature.
[b] Derived from the original data due to the difference in units.

3.1. Metal hydrides

In this section, metal hydrides are summarized and analysed in three catalogues: metal hydrides (e.g., MgH_2, LiH), complex metal hydrides (e.g. $NaAlH_4$, $LiBH_4$), and intermetallic compounds (e.g. LaNi5, TiFe).

3.1.1. Metal hydrides

Lightweight metals including lithium, magnesium, and aluminium have been favourably considered for hydrogen storage due to their higher mass capacity of hydrogen in comparison to heavy metals [69]. It was reported that hydrogen storage capacity in MgH_2 and LiH can be up to 7.65 wt % and 12.78 wt %, respectively [70]. However, the challenges of metal hydrides associate with their high thermodynamic and kinetic barriers. Lithium hydride, with its huge thermodynamic barriers caused by strong ionic bonds, shows hydrogen desorption temperatures of over 800 °C [71]. Aluminium is of broad interest due to its affordability and high recyclability, however, its favourable hydrogen absorption pressure reaches 1000 MPa [72]. In contrast, magnesium hydride offers a myriad of functional properties such as thermal resistance, vibration absorption, reversibility, and recyclability. However, thermodynamic and kinetic challenges persist [69]. For other metals such as sodium, potassium, calcium and zinc, it is also difficult to apply them because of their aggressive chemical properties (e.g., excessively vigorous and rapid reactions with water and air) with the hydrogen storage capacity which is typically less than 1 wt%. A summary of the specific preparation or testing conditions for the hydrides mentioned above is provided in Table 2.

3.1.2. Complex metal hydrides

On-board or other practical mobile operations are beyond the reach of simple metal hydrides owing to their irreversibility and stringent reaction conditions [75]. However, the potential of safe hydrogen storage of such metals motivates researchers to fuse them by ball milling or other means to prepare complex hydrides, such as alanates ($M[BH_4]^-$), borohydrides ($M[AlH_4]^-$) and amides ($M[NH_2]^-$) [76]. Table 3 lists the hydrogen storage capacity and release temperatures of typical alanates, along with their synthesis methods. In general, there are two approaches to make such materials, with one being chemical synthesis and the other being "direct synthesis" which involves the ball-milling of metal hydrides and the corresponding coordination groups [77,78]. The hydrogen release process of complex hydrides typically manifests in multiple stages, each exhibiting distinct kinetic characteristics. This leads to an uneven hydrogen release rate, thereby diminishing the overall reaction kinetics. Generally, the reaction temperature tends to gradually increase across each stage. Therefore, when discussing the overall hydrogen storage capacity, attention is often directed solely towards the temperature required in the final stage, known as the maximum hydrogen release temperature. For instance, the decomposition reaction of NaAlH4 contains two main steps [79].

$$NaAlH_4 \leftrightarrow {}^1\!/\!_3 Na_3AlH_6 + {}^2\!/\!_3 Al + H_2 \quad (1)$$

$$Na_3AlH_6 \leftrightarrow 3NaH + Al + {}^3\!/\!_2 H_2 \quad (2)$$

When the hydrogen and the central atom within the borohydride complex anion are joined through covalent bonding, tetrahydroborates, or borohydrides, are formed. Since a small percent of boron has led to a high proportion of elemental hydrogen by weight in borohydride, it has been emerged as a promising material for hydrogen storage. Table 4 summarises the hydrogen adsorption properties of borohydrides and preparation methods, and highlights the hydrogen resorption capacity.

Although amides show inferior absorption kinetics, their low operation temperatures make them committed towards practical applications. According to Chen et al. [97], hydrogen storage in lithium amides theoretically could reach 7.0 wt % under ~280 °C.

$$Li_2NH + H_2 \leftrightarrow LiNH_2 + LiH \Delta H = -45\ kJ/mol \quad (3)$$

However, the temperature remains excessively high for vehicles and other mobile applications. To further decrease the equilibrium temperature and/or enhance the equilibrium pressure, researchers have explored an alternative approach involving cation displacement to create Li-X-N-H systems. MgH_2 or $Mg(NH_2)_2$ stands out as the most frequently employed material for blending into this system under varying molar ratios of Mg and Li. When Mg and Li are compounded under a 1:2 ratio, the system exhibits hydrogen desorption up to 5.6 wt % at 150 °C through the following reaction [98]:

Table 2
Performance of some typical metal hydrides.

H_2 Storage Material	Gravimetric Capacity (wt %)	Desorption Temperature (°C)	Desorption Pressure (bar)	ΔH (Adsorption, kJ/mol H_2)	Remarks	Ref.
MgH_2	7.65	400	30	−75	Slow adsorption for several hours	[70, 73]
LiH	12.7	825	0.6	−167	High temperature required	[74]
AlH_3	10.1	25	10000	−10	Impractical high pressure	[72]

Table 3
Characteristics of selected alanates.

Material	Gravimetric Capacity (wt. %)	Dehydrogenation Temperature (°C)	ΔH (Adsorption, kJ/mol H_2)	Remarks	Ref.
$NaAlH_4$	7.4	210	−37 (Step 1) −47 (Step 2)	Ziegler's trialkyl aluminium synthesis, aka "Direct Synthesis"	[77, 80]
Na_3AlH_6	5.6	250	−31	H_2 absorption completed after 10 h	[81]
$LiAlH_4$	7.9	220	−37 (Step 1) −45 (Step 2)	High-pressure ball milling 2h with tetrahydrofuran	[82]
$Mg(AlH_4)_2$	9.3	380	−38	Synthesis with diethyl ether	[83]
$KAlH_4$	5.7	380	−35	Synthesis under 270 °C and 175 bar	[84, 85]
$Ca(AlH_4)_2$	7.9	250	−43	Wet-chemical or mechanical synthesis	[78, 86]
Na_2LiAlH_6	3.2	245	−20	Synthesized by ball milling following heat at 150 °C and 50 bar	[87, 88]
K_2NaAlH_6	2.8	325	−30	Prepared by ball-milling before annealing	[89]

Table 4
Characteristics of selected borohydrides.

Material	Hydrogen Capacity (wt. %)	Producing Temperature (°C)	Producing Pressure (bar)	Dehydrogenation Temperature (°C)	Dehydrogenation (wt. %)	Remarks	Ref.
$NaBH_4$	10.8	450–500	3	400	6.5 (@45 °C)	Re-hydrogenation of 5.89 wt % at 600 °C & 4 MPa in 12h	[88, 90]
$LiBH_4$	18.5	550–700	30–150	380	14 (@600 °C)	Reversible capacity of 6.0 wt % H_2 at 350 °C	[91, 92]
$Mg(BH_4)_2$	14.9	–	1	260–400	13.7 (@527 °C)	Reload with 6.1 wt % H_2	[93, 94]
$Ca(BH_4)_2$	11.6	400–440	700	350	9.2 (@527 °C)	5.9 wt % H_2 evolution at 593–650 K & rest 3.5% at around 720 K	[95, 96]

$$2LiNH_2 + MgH_2 \rightarrow Li_2Mg(NH)_2 + 2H_2 \quad (4)$$

3.1.3. Intermetallic hydrides

Intermetallic compounds can be categorized based on their crystal structure and material properties, primarily into AB_5 type rare-earth alloys, AB_2 type Laves-phase alloys, AB type Ti alloys, and Mg-based hydrogen storage alloys. The AB_5 rare-earth hydrogen storage alloy comprises element "A" with a high hydrogen affinity and element "B" with a relatively weak hydrogen affinity. "A" contributes to most of the hydrogen storage capacity and reacts exothermically with hydrogen, whereas "B" is mainly used to improve the reversibility of hydrogen absorption/desorption by regulating the reaction heat as well as the decomposition pressure. A typical example is $LaNi_5$ alloy, its hydride $LaNi_5H_6$ can be easily synthesized under room temperature (~25 °C) and 2 atm pressure [99]. It has been successfully applied and has been noted for its excellent magnetic and electrochemical properties [100].

Laves phase AB_2 alloys, including both Zr-based and Ti-based alloys, such as $ZrMn_2$ and $TiMn_2$, demonstrate high hydrogen storage capacity, optimized hydrogen absorption/desorption kinetics, and minimal hysteresis, etc [101]. However, the remaining challenge is still the limited activation performance and insufficient cycling stability [102].

TiFe, a representative of AB type Ti-based hydrogen storage materials, has been widely studied due to the abundance and cheapness of the feedstock [69]. This material, nevertheless, is comparatively difficult to activate by the presence of a titanium oxide layer, and severe operating conditions are required to reach the maximum theoretical value in cycling (approx. 450 °C, 5 MPa) [103].

Magnesium is recognized as a highly prospective metal for hydrogen storage, with its abundance and non-toxic properties. The hydrogen storage properties of Mg have been systematically investigated by Stampfer's team [104]. Its hydride, MgH_2, has a theoretical hydrogen storage capacity up to 7.6 wt % [70] and an energy density up to 9 MJ/kg Mg [105]. Unfortunately, its high thermodynamic enthalpy and sluggish kinetics have restricted the widespread applications, which is a focal point of current research. The details will be discussed in Chapter Five.

3.2. Carbon-based hydrogen storage material

The major carbon-based materials studied for hydrogen storage are carbon nanotubes (CNTs) including both single-walled nanotubes (SWNTs) and multi-walled nanotubes (MWNTs), graphite nanofibers (GNFs), graphite and graphene, as well as activated carbons (ACs) and porous carbon [106]. These materials leverage the significant surface area and exposed channels of porous materials, exhibiting strong physical adsorption at low temperatures (133K) [107]. However, concerns such as the excessively low operating temperature, for example 77K measured by Masika and Mokaya [108] which is hard to reach, and the difficulties in obtaining nanocarbon materials need to be further addressed.

3.3. Other hydrogen storage materials

Research on other hydrogen storage materials mainly includes metal-organic frameworks (MOFs) and covalent organic frameworks (COFs).

3.3.1. MOF hydrogen storage material

This MOF material boasts a remarkably high surface area (up to 6000 m^2/g) and maintains its structural integrity at high temperatures above 350 °C. Certain hydrogen storage capacity of MOF at low temperatures (77 K) has been discovered, whereas it's hard to performance well under moderate pressures and environmental temperatures [109].

3.3.2. COF hydrogen storage material

COF materials have a similar structure to MOF, characterized by covalent bonds between atoms, enhancing structural stability and eliminating the presence of heavy atoms. Due to its low hydrogen adsorption activity and hydrogen storage capacity (e.g., 0.26 wt % for COF-1 at 25 °C, 100 bar), efforts are switched toward reinforcing its

interaction with hydrogen. Efforts are being made to improve their hydrogen storage performance including modifying pore size, incorporating different metals to create more hydrogen binding sites, etc [110].

4. Mg-based hydrogen storage material

Numerous research has shown that Mg-based hydrogen storage materials not only exhibit promising hydrogen absorption/desorption performance but also, in comparison to most of other materials, can be prepared and utilized under relatively mild conditions. Moreover, Mg is abundant, comprising approximately 2.35% of the crust's overall mass, indicating its cost-effectiveness. Consequently, Mg has attracted great attention, and more than three hundred kinds of Mg-based hydrogen storage materials have been developed to date, covering most of the usual non-metallic elements and most metallic elements, such as Mg–La system, Mg–Ti system and Mg–Fe system.

In addition to forming alloys or second phases with other components, hydrogen can be absorbed directly by Mg. Generally, Mg reacts with high pressure (above 2.4 MPa) hydrogen at temperatures between 300 °C and 400 °C:

$$Mg + H_2 \rightarrow MgH_2 \Delta H = -74.7\ kg/mol \quad (5)$$

The reaction can be reversible under the appropriate conditions (above 400 °C), resulting in a cycle of hydrogen uptake and release. However, there are yet two obstacles to its industrial applications, namely, the high hydrogen release temperature, and its sluggish hydrogen discharge kinetics. Therefore, numerous studies have focused on these issues and proposed measures to improve its thermal stability and hydrogen absorption/desorption kinetics.

4.1. Mechanism of hydrogen storage in Mg-based materials

4.1.1. Hydrogenation and dehydrogenation process

Metal solid solutions (MH_x) and metal hydrides (MH_y) are synthesized through the hydrogenation process involving metals such as Mg under specific temperature and pressure conditions. This reversible phenomenon, known as hydrogenation and dehydrogenation cycling, follows several steps [111]. Initially, hydrogen molecules undergo physisorption and subsequently chemisorption on the alloy surface, leading to the formation of a solid solution through internal diffusion of hydrogen atoms. Upon reaching saturation, excess hydrogen reacts to form metal hydride.

4.1.2. Thermodynamic behaviour

The thermodynamic study of metal hydrides focuses on the thermodynamic equilibrium relationship between the three phases of the metals, the metal hydride as well as the hydrogen at specific temperatures. The thermodynamic of hydrogen storage hydrides, such as isothermal platform pressure and hysteresis of hydrogenation/dehydrogenation process and reversible capacity, can be gained through the pressure-composite-temperature (PCT) curve [112]. The experimental data for the PCT plot can be measured by certain gas analysers, e.g. volumetric high pressure gas adsorber [113], and the principle of it can be evaluated according to the Gibbs' Phase Rule.

$$F = C - P + 2 \quad (6)$$

Where F stands for the degree of freedom of the system, C stands for the number of components and P stands for the number of phases.

The degree of freedom of the system, determined by Gibbs' Phase Rule, influences the hydrogen absorption behaviour at different stages. The relationship between equilibrium hydrogen pressure and temperature at chemical equilibrium can be described by the Van't Hoff equation [114]:

$$\ln\left(\frac{P_{H_2}}{P_0}\right) = \frac{\Delta H}{RT} - \frac{\Delta S}{R} \quad (7)$$

Where P_{H_2} is the corresponding plateau hydrogen pressure at the median hydrogen storage capacity in the PCT curve, P_0 is the standard pressure (1 atm), ΔH is the enthalpy variation of the reaction, ΔS is the entropy variation of the reaction, and R is the gas constant (8.314 J $mol^{-1}\bullet K^{-1}$).

ΔH, a critical parameter for the thermal management of engineering, primarily indicates the stability of the chemical bond formed between the metal and hydrogen, for example, the higher the absolute value of ΔH, the more stable the bond. The majority of hydrogen storage alloys exhibit a negative enthalpy change during hydrogen absorption, indicating that the process of hydrogen uptake is exothermic, coinciding with the formation of M (metal)-H (hydrogen) bonds [115,116]. ΔS, on the other hand, mainly responds to the change in disorder during the transition of hydrogen molecules and solid-solution atoms, and is therefore relatively small in absolute value for most hydrogen storage alloys.

4.1.3. Kinetic behaviour

The kinetics of hydrogen storage alloys focuses primarily on investigating the reaction rates during hydrogen absorption and desorption processes, as well as the energy barriers that must be overcome. Due to the complexity of the actual chemical reactions involved, researchers have proposed various hydrogen storage mechanisms and kinetic equation models for different hydrogen storage alloys. Among the commonly employed kinetic models are the Ginstling-Brounshtein model, which considers interfacial area and diffusion control [117], the Chou model, which is based on interfacial control [118], and the classic John-Mehl-Avrami-Kolmogor (JMAK) nucleation model [119].

4.2. Synthesis of Mg-based material

The present techniques for fabricating Mg-based solid hydrogen storage materials include the ball milling, thin film deposition, hydrogen plasma technology, and liquid-phase reduction method.

4.2.1. Ball milling

Ball milling, a high-energy process, induces continuous fracturing and bonding among powder materials. It is a cost-effective, convenient, and efficient method enabling precise control over the quantitative addition of catalysts to Mg-based hydrides [120]. Ball milling techniques can be categorized into mechanical milling, mechanical alloying, and reactive ball milling.

Mechanical milling, involving ball milling without inducing phase transitions, is employed to prepare nanomaterials or mix different phases [121]. Within the realm of magnesium-based hydrogen storage materials, mechanical milling has been instrumental in generating Mg nanocrystals and composites comprising Mg, catalysts, or other hydrogen storage materials. Liang, Huot [122] conducted experiments to evaluate the hydrogen storage capabilities of MgH_2 combined with various transition metal monomers (Ti, V, Mn, Fe, Ni) after mechanical grinding via ball milling. Their findings revealed that materials incorporating Ti exhibited the most pronounced enhancement in reaction kinetics. Jung, Lee and Lee [123] achieved promising hydrogen storage results at 300 °C through high-energy ball milling of MgH_2 with metal oxides (Cr_2O_3, V_2O_5, Al_2O_3, Fe_2O_3)

Mechanical alloying involves the creation of alloys by blending different metals at the atomic level via prolonged high-energy ball milling. Essentially, it entails the repetitive compression, deformation, crushing, and cold welding of powders. In investigations into magnesium-based hydrogen storage materials, mechanical alloying has been utilized to produce alloys like Mg–Ni, Mg–Co, Mg–Ti, among others. Shao, Asano [124] demonstrated that $Mg_{50}Co_{50}$, synthesized via ball milling in a planetary ball mill at a rotational speed of 200 rpm for

100 h, absorbed 2.67 wt % of hydrogen under a hydrogen pressure of 8 MPa at 258 K. This marks the lowest reported hydrogen absorption temperature for a magnesium-based hydrogen storage material. However, the hydrogen release performance of this storage material at the same temperature is not satisfied, with only 0.47 wt % of hydrogen released.

Reactive ball milling, a method of grinding feedstock in a specific gas atmosphere, is employed in the realm of hydrogen storage materials for the one-step synthesis of monometallic and alloy hydrides. The impact of high-speed grinding balls on the feedstock provides ample energy for chemical reactions at low temperatures, facilitating the synthesis of specialized, typically unstable, metal hydrides. Furthermore, manipulation of the atmosphere composition, the ball-to-feed ratio, and the application of magnetic and electric fields to the ball milling tank allow for the design and preparation of novel hydrides. Shao, Felderhoff and Schüth [125] conducted the synthesis of magnesium-titanium hydride (MgH_2+10mol%TiH_2) composites via reactive ball milling. The raw material comprised a blend of Mg and Ti metal powders with a molar ratio of 10:1, and the initial hydrogen pressure in the ball milling cylinder was maintained at 30 MPa. Monitoring the pressure change revealed a sharp decrease on hydrogen pressure upon the onset of ball milling, indicating rapid hydrogen uptake by Mg and Ti during the early stages of the process. After 3 h, the pressure reached a stable plateau, suggesting the saturation of hydrogen absorption. Differential scanning calorimetry (DSC) analysis of the MgH_2–TiH_2 product indicated a peak hydrogen release temperature of 711 K, which was 96 K lower than that of commercial MgH_2. Table 5 presents a compilation of specific performance parameters corresponding to the examples provided in the three ball milling methods mentioned above.

4.2.2. Thin film forming

Instead of ball milling, the thin-film method offers precise control over the composition, interface, and crystallinity of hydrogen storage materials at nanoscale, thereby providing an effective approach to investigate the hydrogen storage mechanism [126]. While current studies indicate that Mg-based materials necessitate high temperatures for hydrogen storage, thin film materials show potential for enabling Mg-based hydrogen storage materials to operate at room temperature. Qu et al. [127] prepared a series of Pd–Mg thin films with varying thicknesses using direct current sputtering deposition and investigated their hydrogen adsorption kinetics ranging from 298k to 338 K. The study revealed that thinner Mg films, particularly those with thickness below 60 nm, exhibited significantly improved adsorption kinetics under mild conditions, attributed primarily to the formation of MgH_2 at the Pd–Mg interface. The increased thickness of this layer, which caused by the temperature rise or hydrogen pressure drop, pose a significant hindrance to further hydrogen diffusion. The results indicate that the 20 nm Mg film achieved a high storage capacity at up to 5.5 wt% under room temperature (298 K) and 0.7 bar hydrogen pressure.

4.2.3. Direct current arc plasma technology

The direct current arc plasma method relies on the high temperature of the arc to ionize various atoms within the arc column, leading to direct thermal evaporation of the metal. Subsequently, through the plasma generated by various reactive gases such as hydrogen, a series of fundamental processes including metal atom evaporation, gas-phase particle nucleation, nucleus growth, and condensation are undergone to produce metal nanoparticles. Zou et al. conducted the synthesis of a series of composite nano powders comprising Mg and rare earth (RE) elements, including La, Nd, Gd, Y, Ce and Er, using the direct current arc plasma method [128–130]. Through in situ passivation, the rare earth elements within the system underwent transformation into rare earth oxides, such as La_2O_3, Nd_2O_5, Y_2O_3, Ce_2O_3 and Er_2O_3, which were uniformly dispersed and encapsulated on the surface of ultrafine Mg particles, forming a core-shell structure. Additionally, transition metals (TM) like Ti, Ni and Fe were introduced by the team into the binary Mg–La system to further synthesize ternary composite ultrafine powders [131]. The activation energies for hydrogen absorption of Mg–Ti–La, Mg–Ni–La, and Mg–Fe–La were determined as 38.8, 74.48 and 34.47 kJ/mol H_2 respectively, exhibiting superior kinetic properties compared to pure Mg. Notably, Mg–Ni–La displayed outstanding hydrogen uptake rate, achieving hydrogen saturation in approximately 50 s at 573 K and 1 wt % at room temperature within 2 h.

In summary, ball milling offers cost-effective and precise control over catalyst addition, facilitating the preparation of nanomaterials, composites and alloys with improved reaction kinetics. However, it entails high-energy consumption, prolonged processing times, and the challenges like achieving uniform particle size distribution are still exist especially in reactive ball milling. Thin film forming provides precise control at the nanoscale and has potential for room temperature

Table 5
Characteristics of Mg-based alloy/composites prepared by ball-milling.

Material	Temperature (°C)		Pressure (bar)		H_2 Storage Capacity (wt. %)		Time (s)		Remarks	Ref.
	Ads.	Des.	Ads.	Des.	Ads.	Des.	Ads.	Des.		
MgH_2	200	300	10	0.15	4.7	–	1000	1000	Mechanical milling	[122]
MgH_2+5 at%Ti					5.0		50	200		
MgH_2+5 at%V					5.5		50	300		
MgH_2+5 at%Mn					6.0		200	500		
MgH_2+5 at%Fe					4.3		200	300		
MgH_2+5 at%Ni					4.7		1000	400		
MgH_2+5mol%Cr_2O_3	300	–	15	–	4.02	–	600	–	Mechanical milling	[123]
MgH_2+5mol%V_2O_5	250				3.2		600			
MgH_2+5mol%Al_2O_3	300				4.09		600			
					4.49		4000			
MgH_2+5mol%Fe_2O_3	300				1.37		600			
					3.53		5000			
$Mg_{50}Co_{50}$ bcc Alloy	258		80	–	2.67	0.47	–		Mechanical alloying	[124]
	303				2.42	0.39				
	373				2.07	0.33				
MgH_2+10mol%TiH_2	Reactive ball milling synthesis	269	–	0.54	–	5.1	9000	–	Reactive ball milling	[125]
		280		0.75		5.15				
		289		0.98		5.2				
		301		1.39		5.3				
	300	–	100	–	6.5	–	600			
	200		100		4.8		1 h			
	100		100		4		4 h			
	40		100		1.2		5 h			

operation but requires sophisticated equipment and is dependent on the substrate. Direct current arc plasma technology enables the synthesis of composite nano powders with superior kinetic properties, while operates at high temperatures, has limited material versatility and even poses safety concerns.

4.3. Challenges and improvements

Despite the impressive properties of Mg-based hydrogen storage materials, challenges persist, including high activation energies for the dissociation of hydrogen molecules at the surface, low internal hydrogen diffusion rates, and susceptibility to the formation of oxidized layers. Extensive research has focused on addressing these issues through additive catalyst doping, alloying, and nanosizing to enhance hydrogen storage properties.

4.3.1. Effect of catalysts on hydrogen storage performance of Mg-based materials

Doping catalysts represent an effective approach to enhance the hydrogen storage performance of Mg-based materials. The introduction of catalysts serves dual purposes: firstly, it facilitates the dissociation of hydrogen molecules into atoms on adsorption surface, and secondly, it increases the number of diffusion channels for hydrogen. Additionally, this process creates more nucleation sites for the formation of phases during hydrogen adsorption and release. Importantly, the incorporation of a small amount of catalyst does not diminish the hydrogen storage capacity. Various effective catalysts have been studied, including transition metals, transition metal oxides, transition metal halides, rare earth metals and their compounds, as well as carbon-based materials.

Transition metals are recognized as highly effective catalysts, owing to their unique electronic structure. They can form hydrides with hydrogen and function as "spillover" or "hydrogen pumps" during the absorption and release of hydrogen. The term "hydrogen pump" denotes their role in facilitating hydrogen transfer. Transition metal hydrides, which are thermodynamically less stable than pure Mg, initially release hydrogen atoms during hydrogen absorption and release, thus serving as a conduit for hydrogen transfer. "Spillover" refers to a phenomenon where an active centre (primary active centre) on the surface of a solid catalyst adsorbs hydrogen, generating an ionic or radical active species that migrates to another active centre (secondary active centre) [132]. Janot et al. [133] doped Mg_2Ni with 5 wt % Pd via ball milling. During the hydrogen desorption process, the compound with hydrogen (Pd–H) was formed, facilitating the transport of hydrogen from the interior to the exterior of the material. This Pd–H compound acted as a "hydrogen pump", accelerating the migration and diffusion of hydrogen along the crystal boundaries. The spillover mechanism primarily arises from the transition metal phases remaining unchanged during the reaction process. Lu et al. [134] also reported the spillover effect of TiH_2 in the hydrogen adsorption and release process within the ball-milled MgH_2–TiH_2 system.

In the presence of a thin oxide layer on the surface of Mg particles, the metal hydrogenation nucleation reaction is promoted, preventing further oxidation of the Mg substrate [135]. However, with an increase in oxide layer thickness, hydrogen diffusion is impeded, leading to a reduction in the hydrogenation rate. Consequently, transition metal oxides have also garnered significant attention from researcher. Oelerich et al. [136] utilized a high-energy ball milling method to incorporate transition metal oxides (TM_xO_y, including TiO_2, V_2O_5, Cr_2O_3, Mn_2O_3, Fe_3O_4, CuO, Al_2O_3, Sc_2O_3, SiO_2, etc.) into the MgH_2 system. Through an examination of the properties of the resulting MgH_2-TM_xO_y composite, it was determined that multivalent transition metal oxides (such as TiO_2, V_2O_5, Cr_2O_3, Mn_2O_3, Fe_3O_4) exhibit significantly superior catalytic effects compared to single-valence metal oxides (e.g., Al_2O_3, Sc_2O_3, SiO_2). Multivalent transition metal ions undergo valency changes during hydrogen absorption and discharge, forming oxides with varying stoichiometric ratios. This enhances the electron exchange reaction with hydrogen molecules, creates more pathways for hydrogen atom diffusion, and hence improves the kinetic performance of the material.

Transition metal fluorides (TMF_x) and chlorides ($TMCl_y$) also have been identified as effective catalysts for enhancing the kinetic properties of hydrogen absorption and desorption in Mg-based materials. Transition metal fluorides (NiF_2, TiF_3, VF_4, NbF_5, FeF_2, ZrF_4, CrF_2) were introduced into MgH_2 via ball milling, and an extensive investigation revealed their significant impact on reducing the hydrogen release temperature and improving the kinetics of hydrogen uptake when cycling [137]. This effect principally stems from the reaction between TMF_x and MgH_2, resulting in the formation of metal hydrides or hydrogen solid solutions during the ball milling process. First-principle calculations further demonstrate that the synergistic catalytic effect of Ti and F on the hydrogen storage properties of MgH_2 is attributed to the presence of TiH_2 and MgF_2 during the reaction process, which surpasses the catalytic effect of individual Ti and F elements [138]. Similarly, through mechanical ball milling, Malka's team investigated transition metal chlorides ($NbCl_5$, $ZrCl_4$, $CdCl_2$, $TiCl_3$, VCl_3, $CrCl_2$, $CrCl_3$) and examined the hydrogen storage properties of the systems formed with MgH2 [139]. Among these, $TiCl_3$ and VCl_3 exhibited the most promising catalytic properties. $TiCl_3$, in particular, undergoes a disproportionation reaction during the process, generating a substantial number of defects that significantly enhance the hydrogen storage properties. The BET (Brunauer-Emmett-Teller) test further revealed that after ball milling, the specific surface area of the MgH_2+7 wt % $TiCl_3$ composite material can reach 24.3 m^2/g [140].

The high specific surface area of carbon nanomaterials (SWNT, MWNT, activated carbon, graphite, graphene, etc.) along with their inherent hydrogen adsorption capabilities have rendered them focal points in catalyst research of Mg-based materials. Konarova et al. [141] prepared porous MgH_2/C composite hydrogen storage materials by heating porous carbon and $MgBu_2$ under 2 MPa hydrogen pressure at various temperatures, with the best-performing batch achieving a hydrogen absorption capacity of 6 wt % within 3 min at 250 °C. Liu et al. [142] conducted a detailed analysis of the superior hydrogen storage performance of graphene/MgH_2 materials after ball milling, attributing it to the provision of additional edge sites and hydrogen diffusion channels by graphene, which also impedes the growth and agglomeration of nanoparticles during hydrogen absorption/desorption cycles. Additionally, MgH_2 doped with 5 wt% Co + 5 wt % MWNTs achieved a hydrogen re-absorption capacity of 6.5 wt % within 100 s at 250 °C, with complete hydrogen release within 85 min, owing to the synergistic catalytic effect by Co and MWNTs [143].

4.3.2. Effect of alloying on hydrogen storage performance of Mg-based materials

Through alloying with various elements, certain phases of hydrides can be formed based on Mg, thereby enhancing the hydrogen storage capabilities of Mg-based materials. The elements investigated for alloying with Mg predominantly include transition metals (TM = Fe, Co, Ni, Cu, etc.) and rare earth metals (RE = La, Ce, Nd, etc.).

4.3.2.1. Mg-TM alloy. The Mg–Ni alloy is one of the most extensively studied and earliest investigated hydrogen storage alloys. The earliest Mg–Ni alloy was synthesized by Reilly et al. using an induction furnace under an argon atmosphere, and their team systematically studied the hydrogen storage performance of this system [144]. According to the Mg–Ni phase diagram, two phases exist between them, Mg_2Ni and $MgNi_2$. Among them, the $MgNi_2$ phase cannot form hydrides, whereas the Mg_2Ni phase can form the hydride Mg_2NiH_4, with a formation enthalpy of −64.6 kJ/mol H_2 and a theoretical hydrogen storage capacity of 3.6 wt % H_2 [145]. This indicates that thermodynamically, Mg_2NiH_4 is more prone to decomposition compared to MgH_2. However, due to its lower theoretical hydrogen storage capacity, as mentioned earlier, it cannot meet the final requirements of the U.S. DOE for

onboard hydrogen storage systems. Therefore, more research is focused on combining MgH_2 and Mg_2NiH_4 through various methods to increase the hydrogen storage capacity of the alloy system while also reducing its thermal stability. Mg–Co alloys have the capability to form the Mg_2CoH_5 phase under hydrogen pressures ranging from 4 to 6 MPa and temperatures exceeding 350 °C. Theoretical calculations indicate a hydrogen storage capacity of 4.5 wt % H_2 with an enthalpy of formation of −86 kJ/mol H_2. Despite its relatively high value of enthalpy, combining Mg–Co alloys with MgH_2 can effectively enhance the hydrogen storage performance while reducing the stability of the hydrogen storage system [146]. Two phases, $MgCu_2$ and Mg_2Cu, could also be formed by Mg–Cu, where the former exhibits negligible hydrogen absorption, while the latter, under conditions of 240 °C and 0.1 MPa hydrogen pressure, facilitates the formation of MgH_2 from Mg, concurrently generating the $MgCu_2$ phase [147]. This occurrence diminishes the overall reversibility and potential utility of the hydrogen storage system. There is no thermodynamic equilibrium intermetallic compound between Mg and Fe. However, when Mg and Fe are mixed at a molar ratio of 2:1 and subjected to conditions of 400 °C and 3 MPa for 10 min, the Mg_2FeH_6 phase can be hydrogenated. Under these conditions, the Mg_2FeH_6 phase exhibits favourable hydrogen storage properties, reaching 5.44 wt % H, close to the theoretical value of 5.5 wt % H [148].

4.3.2.2. Mg-RE alloy. The RE elements investigated for alloying predominantly include lanthanides (Ln), encompassing elements like lanthanum (La), praseodymium (Pr), cerium (Ce), neodymium (Nd), among others. Alloys of Mg with these RE elements, such as $LnMg_{12}$, Ln_2Mg_{17}, Mg_3Ln, etc., can serve as hydrogen storage materials. Notably, $CeMg_{12}$, $LaMg_{12}$, and LaM_{17} exhibit hydrogen storage capacities of 6, 4.5, and 6.63 wt % H_2, respectively. While they demonstrate promising hydrogen absorption kinetics at room temperature post-activation, their elevated dehydrogenation temperatures pose challenges for practical applications [149–152].

4.3.3. Effect of nanosizing on hydrogen storage performance of Mg-based materials

Nanotechnology is pivotal for optimising the hydrogen storage capability of Mg-based materials. Nanomaterials, typically sized between 1 and 100 nm, exhibit unique properties due to their high surface area-to-volume ratio. This phenomenon, known as surface, effects, enhances chemical reactivity and catalytic activity. Specifically, nanoparticles with surface atoms comprising a significant proportion of the total atoms demonstrate heightened reactivity, making them effective in promoting chemical reactions as reactants (i.e., Mg nano powder) or catalysing hydrogen-related processes in Mg-based hydrogen storage materials [153].

Additionally, nanomaterials harbour abundant grain boundaries, which provide more pathways for hydrogen atom diffusion. Moreover, the unique size effects of nanomaterials shorten the diffusion distance of hydrogen atoms, accelerating the hydrogen storage process. Currently, methods for preparing nanostructured Mg-based hydrogen storage materials mainly include high-energy ball milling, vapor/liquid/solid-phase methods, and nanoconfinement approaches.

5. Porous structure in Mg-based material

Diverse morphologies of substrate materials in hydrogen storage, such as bulk, powder or nanoscale powders, can significantly influence their storage capabilities. Similarly, the morphology and the adhesion structure of catalysts, for example in the presence of nanoparticles, thin films or core-shell structures, exhibit varied catalytic properties. Porous materials, in turn, represent a major avenue of structural exploration. Recently, solid-state porous hydrogen storage materials and their associated composites have attracted significant attention. Beyond the ubiquitous advantages of porous materials, including large surface area and elevated porosity, their peculiar attributes are of paramount significance, encompassing customizable specific pores and adsorption environments, prominent computationally structural features, and exceptional controllability. Specifically, metal-organic frameworks (MOFs), covalent organic frameworks (COFs), porous organic polymers (POPs), carbon-based materials, zeolites, and their derivatives that embedded by light-element hydrides have been extensively investigated for hydrogen storage applications [154]. Among these, studies have focused on structural improvements of Mg-based materials. In addition to the hydrogen storage materials, there are abundant applications of porous magnesium materials in the realm of biomaterials. Moreover, researchers have delved deeper into material rigidity and corrosion resistance, offering valuable insights for further exploration of Mg based materials for hydrogen storage.

5.1. Porous Mg-based film

Porous Mg-based thin films, a promising technique, exhibit a "film thickness effect" during hydrogen absorption. Ham and co-workers achieved the deposition of dense Mg films (200 nm) and thicker porous Mg films (ranging from 400 nm to 1600 nm) by growing films on SiO_2 substrates using DC (Direct Current) magnetron sputtering [155]. A decrease in hydrogen storage performance with increasing film thickness was observed, possibly due to the presence of metastable MgH_2 phases. Additionally, Mg nanopillars were fabricated by rotating the silicon base by 5° and 45°, revealing superior pore densification and hydrogen storage performance at a tilt angle of 45°. Xin et al. varied the substrate temperature of silicon-based chips (25 °C, 80 °C, 120 °C, and 150 °C) under negative-pressure argon gas conditions and utilized direct current magnetron sputtering technology to fabricate Pd–Mg thin films (10 nm Pd layer deposited on a 200 nm Mg layer) [156]. Surface and cross-sectional SEM (Scanning Electron Microscope) images revealed that as the temperature of the silicon chips increased, the Mg–Pd thin film transitioned from dense to porous morphology. Comparing the rate of resistance change (R/R_0, where R_0 is the resistance value in the non-hydrogenated state and R is the instantaneous resistance that varies with hydrogenation time), it was observed that the hydrogen absorption kinetics were exceptionally slow for the low-temperature fabricated Mg–Pd films (25 °C and 80 °C), while the opposite trend was observed for the high-temperature group (120 °C and 150 °C), showing a significantly increased rate. The hydrogen absorption rate as well as the capacity of the sample prepared 150 °C are notably outstanding, approaching the theoretical H_2 storage limit of pure Mg (7.6 wt %) within a short period (10 min) under 353 K. The excellent performance of the porous Mg–Pd film can be attributed to the accelerated mass transfer of hydrogen from the surface to the interior due to the presence of pores, along with increased reactive surface area of the active metal nanoparticles. However, once subjected to hydrogen absorption and desorption cycling (300 K, hydrogen absorption/desorption pressure of 0.5 bar and 10 Pa respectively), the performance of the film significantly deteriorated. Except for the 150 °C group, which barely maintained a hydrogen absorption and desorption amount of approximately 2 wt % in the third cycle, the other temperature groups failed to complete even the second desorption cycle.

5.2. MOF with Mg site

Zhou and co-authors reported a systematic investigation on the H_2 adsorption of a series of isostructural MOFs, termed M-MOF-74 (M = Mg, Mn, Co, Ni, Zn). These MOFs, possessing open metal sites, manifested an enhanced H_2 bonding strength compared to classical MOFs, attributed to the direct and robust interaction between H_2 and the coordinating unsaturated metal ions [157]. In the same year, a range of structural isomerism of MOF-74, known as M_2 (*m*-dobdc), 4,6-dioxido-1, 3-benzenedicarboxylate was conducted by Long et al., to enhance the charge density and augment the H_2 bonding capabilities of MOFs [158].

Through experimental analysis, it was observed that M_2 (*m*-dobdc) (M = Mg, Ni, Co, Fe, Mn), featuring open metal sites with intensified charge density, exhibits elevated H_2 bonding enthalpies compared to M-MOF-74 due to alterations in the coordination field at the metal sites.

5.3. Zeolite templated Mg-based materials

Zeolites, $M_{\frac{1}{n}}^{n+}(AlO_2)^{-}(SiO_2)_x \bullet yH_2O$ where $M_{\frac{1}{n}}^{n+}$ is the metal or hydrogen ions that can exchange with other cations in the electrolyte solution, are aluminosilicate minerals with a framework structure containing numerous cavities and interconnected channels [159]. However, the presence of counter ions, a common component within zeolite structures, hinders their ability to bond with external adsorbate molecules. Moreover, porous hydrogen storage materials typically require high porosity, contrary to zeolites which consist of relatively heavy elements. Consequently, research on hydrogen storage using zeolites is limited. Langmi et al. [160] investigated the utilization of zeolites A, X, Y and RHO, considering their diverse compositions and geometric pore shapes. Under optimal conditions (77 K, 15 bar), MgY exhibited a hydrogen storage capacity of 1.74 wt %. Similarly, under the same conditions, NaX and NaY demonstrated hydrogen storage capacities of 1.79 wt % and 1.81 wt %, respectively.

5.4. Mg-based materials under nanoconfinement

In addition to manipulating the framework structure itself, there is also significant performance enhancement by utilizing rigid porous frameworks to confine and immobilize light metal hydrides. Leick and colleagues employed a nano-encapsulation strategy coupled with chemical admixtures to enhance magnesium borohydride, $Mg(BH_4)_2$, which boasts one of the highest hydrogen storage capacities (around 14.9 wt %) among metal hydrides. Through atomic layer deposition (ALD) techniques utilizing Al_2O_3, the study demonstrated a doubling of hydrogen storage capacity at low temperatures compared to $Mg(BH_4)_2$ without Al_2O_3 additives [161]. Additionally, the desorption kinetics were significantly optimized, showing effective performance within 100 cycles, for example, impeding the formation of the by-product diborane.

The research from Allendorf investigated the incorporation of $Mg(BH_4)_2$ into the pores of a UiO-67bpy MOF linkers via solvent impregnation [162]. The maintenance of the original MOF structure was illustrated, indicating a uniform partitioning of hydrides. X-ray absorption spectroscopy (XAS) corroborated Mg coordination, while in-situ experiments demonstrated the entire hydrogen desorption at 200 °C with the improved kinetics. These findings suggest potential for low-temperature hydrogen release, proved by calculations from density functional theory showing reduced activation energy for B–H bond disassociation. Besides, MOF nodules could as well help to identify and immobilize externally applied metal nanocompound materials. Zou et al. [163] demonstrated the preparation of MgH_2@Ni-MOF composites via solvothermal and wet-impregnation techniques, resulting in enhanced hydrogen adsorption properties of MgH_2. The Ni-MOF holder effectively inhibited the crystal development and clustering of Mg/MgH_2 nanocrystals, attributed to improved system cycling steadiness. Overall, the integration of lightweight metal materials with MOFs represents a clever design strategy, offering robust tunability and a wide range of material choices. However, challenges persist in the practical application of such composites in hydrogen storage environments, particularly concerning heat resistance and material overloading.

A number of porous hollow carbon nanospheres (HCNs) with diverse mesopore sizes and thicknesses over carbon crusts were synthesized as scaffolds through the nickel template approach, which then were mixed with Cp2Mg and THF in argon to obtain the ultimate Mg composite hydrogen storage material in the confines of the nano-framework [164]. The results indicate that such HCN/Mg nanocomposites feature large pores (5.20, 6.19, and 13.06 nm), along with improved kinetic and thermodynamic properties for hydrogen storage than conventional Mg nanoconfined materials with smaller pores. A finer kinetic analysis revealed that the composites possessing thick carbon shells exerted greater compressive strains on the confined Mg, thus rendering the absorption/desorption of hydrogen intractable. Further calculations by the authors suggested that the compressive stress moderated the inward hydrogen diffusion within the material, however accelerating the surface dehydrogenation rate.

6. Conclusion and outlook

This paper provides a comprehensive overview of recent research progress of Mg-based materials in the field of hydrogen storage. Existing hydrogen storage methods are systematically classified and reviewed individually and the potential of Mg-based materials in hydrogen storage is analysed progressively. The thermodynamic and kinetic performance of Mg-based materials, synthesis methods including ball milling, thin film deposition, direct current plasma technology, etc., as well as the properties of synthesized Mg-based alloys/composite materials are discussed. The challenges and existing solutions are summarized, including methods such as doping catalysts, alloying, and nanostructuring to improve the hydrogen storage performance. MgH_2/Mg system shows better performance under the nano-confinement of Ni-MOF materials by not only improving the catalytic efficiency, but also greatly increasing the rigidity and cycling stability. The final focus of the paper is on porous materials, with an aim for further research and exploration in this direction.

From a material science perspective, it can be noted that improving surface area is critical to accelerate the hydronation and dehydration, one possible way is template-based fabrication which has been used in Mg-based biomaterials. The fabrication of porous Mg-based scaffolds typically relies on specific spatial supporting materials, such as metals, salts, and even gases. Jiang et al. [165] referred to a method for fabricating Mg-skeletons with Ti filaments as a space-holding material. By dosing molten Mg into Ti wires structured as a three-dimensional cage-like lattice to form the Ti/Mg blend system, the final resulting porous Mg scaffolds was then obtained by hydrofluoric acid (HF) erosion of the Ti. Characterization results revealed that the porosity of the Mg frameworks reached 43.2%, 51%, and 54.2%, respectively, with pores consisting of tubular channels approximately 270 μm in diameter. The pore size and structure of the material prepared by this method can be intentionally controlled. Additionally, mechanical testing demonstrated that the resultant porous Mg exhibited elastic moduli of 1.0, 0.6, and 0.5 GPa for the aforementioned porosities, respectively, with compressive yield strengths of 6.2, 4.6, and 4.3 MPa. Such materials with outstanding mechanical properties can serve as a valuable reference for hydrogen storage materials, aiming to enhance material stability during hydrogen absorption/desorption cycles while reducing the likelihood of agglomeration. Another example, bio-inspired flow field designs mimicking leaf vein structures significantly improved fuel cell performance [166]. Applying these designs to hydrogen fuel cells, in combination with solid-state hydrogen storage technologies, could enhance hydrogen utilization and round-trip efficiency.

Besides, leveraging high-performance AI (Artificial Intelligence) and various advanced models can assist in accurately computing, predicting, and analysing the optimal solutions for structure and composition ratios. The hydrogen affinity portion should be additionally considered and incorporated into existing porous structures. From an engineering perspective, the overall energy utilization efficiency of the system, including the hydrogen storage capacity and the amount of external energy applied, is far more critical than the hydrogen storage performance at the molecular or crystal level. When materials are used on a large scale, their stability, porosity, mass and heat transfer parameters will be inferior to those measured at the laboratory scale. Therefore, advanced 3D printing technologies, template-filled calcination methods, or chemical adhesives should be further investigated. Meanwhile, under

long-term hydrogen cycling, promoting the heat recovery of each hydrogen absorption and desorption cycle is particularly essential, which will significantly improve the overall system energy utilization efficiency after thousands of cycles.

Additionally, cost control is imperative before large-scale industrialization, necessitating future research to avoid focusing solely on rare earth elements or extremely advanced and scarce materials. Chen et al. [167] developed the conventional alloy casting method to process common Mg–Ni alloys with ultrasonic treatment, yielding materials with remarkable refinement and uniformity in microstructure, and highly enhanced hydrogen-absorbing capacity and rate. Such improvements in manufacturing techniques, achieving comparable results to those obtained by adding expensive metals, are likely to be widely adopted in the future.

CRediT authorship contribution statement

Haoliang Hong: Writing – original draft, Data curation. **Hangzuo Guo:** Writing – original draft, Data curation. **Zhanfeng Cui:** Writing – review & editing. **Anthony Ball:** Writing – review & editing. **Binjian Nie:** Writing – review & editing, Funding acquisition, Conceptualization.

Declaration of competing interest

The authors declare that they have no known competing financial interests or personal relationships that could have appeared to influence the work reported in this paper.

Acknowledgement

The work is supported by University of Oxford Challenge Research Fund (UCSF490) and EPSRC New Investigator Award (EP/Y015924/1).

References

[1] Chen LM, et al. Embodied energy intensity of global high energy consumption industries: a case study of the construction industry. Energy 2023;277:13.
[2] Mossie AT, et al. Investigating energy saving and climate mitigation potentials in cement production – a case study in Ethiopia. Energy Convers Manag 2023;287:117111.
[3] Wang Z, et al. Synergy of carbon capture, waste heat recovery and hydrogen production for industrial decarbonisation. Energy Convers Manag 2024;312:118568.
[4] Nauman A, et al. Minimizing energy consumption for NOMA multi-drone communications in automotive-industry 5.0. Journal of King Saud University - Computer and Information Sciences 2023;35(6):101547.
[5] Arto I, et al. The energy requirements of a developed world. Energy for Sustainable Development 2016;33:1–13.
[6] Jabbr AI, Gaja H, Koylu UO. Multi-objective optimization of operating parameters for a H2/Diesel dual-fuel compression-ignition engine. Int J Hydrogen Energy 2020;45(38):19965–75.
[7] Jabbr AI, Koylu UO. Influence of operating parameters on performance and emissions for a compression-ignition engine fueled by hydrogen/diesel mixtures. Int J Hydrogen Energy 2019;44(26):13964–73.
[8] Fan Z, et al. Catalytic decomposition of methane to produce hydrogen: a review. J Energy Chem 2021;58:415–30.
[9] Lee JE, et al. Catalytic ammonia decomposition to produce hydrogen: a mini-review. Chem Eng J 2023;475:146108.
[10] Musa Ardo F, et al. A review in redressing challenges to produce sustainable hydrogen from microalgae for aviation industry. Fuel 2022;330:125646.
[11] Muthukumar P, et al. Review on large-scale hydrogen storage systems for better sustainability. Int J Hydrogen Energy 2023;48(85):33223–59.
[12] Wang, R., et al., A critical review for hydrogen application in agriculture: recent advances and perspectives. Crit Rev Environ Sci Technol: p. 1-17.
[13] Papageorgiou C, Saam M, Schulte P. Substitution between clean and dirty energy inputs: a macroeconomic perspective. Rev Econ Stat 2017;99(2):281–90.
[14] Black R, et al. Taking Stock: a global assessment of net zero targets. Energy & climate intelligence unit and oxford net zero 2021;23.
[15] Yang F, et al. Review on hydrogen safety issues: Incident statistics, hydrogen diffusion, and detonation process. Int J Hydrogen Energy 2021;46(61):31467–88.
[16] Najjar YSH. Hydrogen safety: the road toward green technology. Int J Hydrogen Energy 2013;38(25):10716–28.
[17] Moradi R, Groth KM. Hydrogen storage and delivery: review of the state of the art technologies and risk and reliability analysis. Int J Hydrogen Energy 2019;44(23):12254–69.
[18] Chandra Muduli R, Kale P. Silicon nanostructures for solid-state hydrogen storage: a review. Int J Hydrogen Energy 2023;48(4):1401–39.
[19] Ali NA, Sazelee NA, Ismail M. An overview of reactive hydride composite (RHC) for solid-state hydrogen storage materials. Int J Hydrogen Energy 2021;46(62):31674–98.
[20] Andersson J, Grönkvist S. Large-scale storage of hydrogen. Int J Hydrogen Energy 2019;44(23):11901–19.
[21] Hassan IA, et al. Hydrogen storage technologies for stationary and mobile applications: review, analysis and perspectives. Renew Sustain Energy Rev 2021;149:111311.
[22] Hwang HT, Varma A. Hydrogen storage for fuel cell vehicles. Current Opinion in Chemical Engineering 2014;5:42–8.
[23] Zhang T, et al. Hydrogen liquefaction and storage: recent progress and perspectives. Renew Sustain Energy Rev 2023;176:113204.
[24] Elberry AM, et al. Large-scale compressed hydrogen storage as part of renewable electricity storage systems. Int J Hydrogen Energy 2021;46(29):15671–90.
[25] Lang C, Jia Y, Yao X. Recent advances in liquid-phase chemical hydrogen storage. Energy Storage Mater 2020;26:290–312.
[26] Pedicini R, et al. Hydrogen storage based on polymeric material. Int J Hydrogen Energy 2011;36(15):9062–8.
[27] Ramimoghadam D, Gray EM, Webb CJ. Review of polymers of intrinsic microporosity for hydrogen storage applications. Int J Hydrogen Energy 2016;41(38):16944–65.
[28] Vasiliev LL, et al. Activated carbon and hydrogen adsorption storage. In: NATO advanced research Workshop on hydrogen materials science and Chemistry of carbon nanomaterials. Sevastopol, UKRAINE; 2005.
[29] Jin J, Ouyang J, Yang H. Pd nanoparticles and MOFs synergistically hybridized halloysite nanotubes for hydrogen storage. Nanoscale Res Lett 2017;12(1):240.
[30] Klontzas E, Tylianakis E, Froudakis GE. Designing 3D COFs with enhanced hydrogen storage capacity. Nano Lett 2010;10(2):452–4.
[31] Tarasov BP, et al. Metal hydride hydrogen storage and compression systems for energy storage technologies. Int J Hydrogen Energy 2021;46(25):13647–57.
[32] Umegaki T, et al. Boron- and nitrogen-based chemical hydrogen storage materials. Int J Hydrogen Energy 2009;34(5):2303–11.
[33] Bezdudny AV, Blinov DV, Dunikov DO. Single-stage metal hydride-based heat storage system. J Energy Storage 2023;68:107590.
[34] Dong Z, et al. A design methodology of large-scale metal hydride reactor based on schematization for hydrogen storage. J Energy Storage 2022;49:104047.
[35] Ji X, et al. Probing the electrochemical capacitance of MXene nanosheets for high-performance pseudocapacitors. Phys Chem Chem Phys 2016;18.
[36] Bowman RC, Fultz B. Metallic hydrides I: hydrogen storage and other gas- phase applications. MRS Bull 2002;27(9):688–93.
[37] Bhouri M, et al. Honeycomb metallic structure for improving heat exchange in hydrogen storage system. Int J Hydrogen Energy 2011;36(11):6723–38.
[38] Fakioğlu E, Yürüm Y, Nejat Veziroğlu T. A review of hydrogen storage systems based on boron and its compounds. Int J Hydrogen Energy 2004;29(13):1371–6.
[39] Aziz M, Wijayanta AT, Nandiyanto ABD. Ammonia as effective hydrogen storage: a review on production, storage and utilization. Energies 2020;13(12):3062.
[40] Bano S, et al. Hydrogen transportation using liquid organic hydrides: a comprehensive life cycle assessment. J Clean Prod 2018;183:988–97.
[41] Biniwale RB, et al. Chemical hydrides: a solution to high capacity hydrogen storage and supply. Int J Hydrogen Energy 2008;33(1):360–5.
[42] Tarasov BP, et al. Metal hydride hydrogen compressors for energy storage systems: layout features and results of long-term tests. J Phys: Energy 2020;2(2):024005.
[43] Lototskyy MV, et al. The use of metal hydrides in fuel cell applications. Prog Nat Sci: Mater Int 2017;27(1):3–20.
[44] Han G, et al. Development of a high-energy-density portable/mobile hydrogen energy storage system incorporating an electrolyzer, a metal hydride and a fuel cell. Appl Energy 2020;259:114175.
[45] Baricco M, et al. SSH2S: hydrogen storage in complex hydrides for an auxiliary power unit based on high temperature proton exchange membrane fuel cells. J Power Sources 2017;342:853–60.
[46] Lamb KE, Webb CJ. A quantitative review of slurries for hydrogen storage – slush hydrogen, and metal and chemical hydrides in carrier liquids. J Alloys Compd 2022;906:164235.
[47] Liu H, et al. Aluminum hydride for solid-state hydrogen storage: structure, synthesis, thermodynamics, kinetics, and regeneration. J Energy Chem 2021;52:428–40.
[48] Sazelee NA, Ismail M. Recent advances in catalyst-enhanced LiAlH4 for solid-state hydrogen storage: a review. Int J Hydrogen Energy 2021;46(13):9123–41.
[49] Ruslan N, et al. Review on magnesium hydride and sodium borohydride hydrolysis for hydrogen production. Crystals 2022;12(10):1376.
[50] Dragan M. Hydrogen storage in complex metal hydrides NaBH4: hydrolysis reaction and experimental strategies. Catalysts 2022;12(4):356.
[51] Gor Bolen M. Hydrogen storage in porous silicon – a review. Silicon 2023;15(11):4663–73.
[52] Zhao D, et al. Porous metal–organic frameworks for hydrogen storage. Chem Commun 2022;58(79):11059–78.
[53] Kopac T. Hydrogen storage characteristics of bio-based porous carbons of different origin: a comparative review. Int J Energy Res 2021;45(15):20497–523.

[54] Li Q, et al. Thermodynamics and kinetics of hydriding and dehydriding reactions in Mg-based hydrogen storage materials. J Magnesium Alloys 2021;9(6):1922–41.
[55] Shang Y, et al. Mg-based materials for hydrogen storage. J Magnesium Alloys 2021;9(6):1837–60.
[56] Yang Y, et al. Recent advances in catalyst-modified Mg-based hydrogen storage materials. J Mater Sci Technol 2023;163:182–211.
[57] Ali NA, Ismail M. Advanced hydrogen storage of the Mg–Na–Al system: a review. J Magnesium Alloys 2021;9(4):1111–22.
[58] Ding X, et al. Recent progress on enhancing the hydrogen storage properties of Mg-based materials via fabricating nanostructures: a critical review. J Alloys Compd 2022;897:163137.
[59] Ren L, et al. Nanostructuring of Mg-based hydrogen storage materials: recent advances for promoting key applications. Nano-Micro Lett 2023;15(1):93.
[60] Eberle U, Felderhoff M, Schueth F. Chemical and physical solutions for hydrogen storage. Angew Chem Int Ed 2009;48(36):6608–30.
[61] Stetson N. An overview of US DOE's activities for hydrogen fuel cell technologies. In: Proceedings of the materials challenges in alternative & renewable energy conference; 2012.
[62] Rivard E, Trudeau M, Zaghib K. Hydrogen storage for mobility: a review. Materials 2019;12(12):1973.
[63] Moreno-Blanco J, et al. The storage performance of automotive cryo-compressed hydrogen vessels. Int J Hydrogen Energy 2019;44(31):16841–51.
[64] Sirosh N, Corbin R, Niedzwiecki A. Hydrogen composite tank project. Progress report department of energy. US government; 2003.
[65] Langmi HW, et al. Hydrogen storage. In: Electrochemical power sources: fundamentals, systems, and applications. Elsevier; 2022. p. 455–86.
[66] Ashton E, et al. Evaluation of the vapor hydrolysis of lithium aluminum hydride for mobile fuel cell applications. ACS Appl Energy Mater 2022;5(7):8336–45.
[67] Zhao D, et al. Porous metal-organic frameworks for hydrogen storage. Chem Commun 2022.
[68] Vudumu SK, Koylu UO. Detailed simulations of the transient hydrogen mixing, leakage and flammability in air in simple geometries. Int J Hydrogen Energy 2009;34(6):2824–33.
[69] Sakintuna B, Lamari-Darkrim F, Hirscher M. Metal hydride materials for solid hydrogen storage: a review. Int J Hydrogen Energy 2007;32(9):1121–40.
[70] Selvam P, et al. Magnesium and magnesium alloy hydrides. Int J Hydrogen Energy 1986;11(3):169–92.
[71] Jain A, Miyaoka H, Ichikawa T. Destabilization of lithium hydride by the substitution of group 14 elements: a review. Int J Hydrogen Energy 2016;41(14):5969–78.
[72] Jiang W, Wang H, Zhu M. AlH3 as a hydrogen storage material: recent advances, prospects and challenges. Rare Met 2021;40(12):3337–56.
[73] Zaluska A, Zaluski L, Ström–Olsen JO. Nanocrystalline magnesium for hydrogen storage. J Alloys Compd 1999;288(1):217–25.
[74] Messer CE. A survey report on lithium hydride, 9470. United States Atomic Energy Commission; 1960. Technical Information Service.
[75] Liu Y, et al. Development of catalyst-enhanced sodium alanate as an advanced hydrogen-storage material for mobile applications. Energy Technol 2018;6(3):487–500.
[76] Zhao L, et al. Enhanced hydrogen storage of alanates: recent progress and future perspectives. Prog Nat Sci: Mater Int 2021;31(2):165–79.
[77] Ziegler K, et al. Metallorganische Verbindungen, XXVI Aluminiumtrialkyle und Dialkyl-Aluminiumhydride aus Olefinen, Wasserstoff und Aluminium. Justus Liebigs Ann Chem 1960;629(1):1–13.
[78] Fichtner M, Frommen C, Fuhr O. Synthesis and properties of calcium alanate and two solvent adducts. Inorg Chem 2005;44(10):3479–84.
[79] Balogh MP, et al. Phase changes and hydrogen release during decomposition of sodium alanates. J Alloys Compd 2003;350(1):136–44.
[80] Bogdanović B, et al. Metal-doped sodium aluminium hydrides as potential new hydrogen storage materials. J Alloys Compd 2000;302(1):36–58.
[81] Ashby EC, Kobetz P. The direct synthesis of Na3AlH6. Inorg Chem 1966;5(9):1615–7.
[82] Wang J, Ebner A, Ritter J. Physiochemical pathway for cyclic dehydrogenation and rehydrogenation of LiAlH 4. J Am Chem Soc 2006;128:5949–54.
[83] Fichtner M, Fuhr O, Kircher O. Magnesium alanate—a material for reversible hydrogen storage? J Alloys Compd 2003;356–357:418–22.
[84] Dymova TN, et al. Direct synthesis of alcali metal alumohydrides in melts. Dokl Akad Nauk SSSR 1974;215(6):1369–72.
[85] Morioka H, et al. Reversible hydrogen decomposition of KAlH4. J Alloys Compd 2003;353(1):310–4.
[86] Mamatha M, et al. Comparative studies of the decomposition of alanates followed by in situ XRD and DSC methods. J Alloys Compd 2006;416(1–2):303–14.
[87] Brinks HW, et al. Synthesis and crystal structure of Na2LiAlD6. J Alloys Compd 2005;392(1):27–30.
[88] Jain IP, Jain P, Jain A. Novel hydrogen storage materials: a review of lightweight complex hydrides. J Alloys Compd 2010;503(2):303–39.
[89] Sørby MH, et al. The crystal structure and stability of K2NaAlH6. J Alloys Compd 2006;415(1):284–7.
[90] Çakanyıldırım Ç, Gürü M. Hydrogen cycle with sodium borohydride. Int J Hydrogen Energy 2008;33(17):4634–9.
[91] Ozturk T, Demirbas A. Boron compounds as hydrogen storage materials. Energy Sources, Part A Recovery, Util Environ Eff 2007;29(15):1415–23.
[92] Zhang Y, et al. LiBH4 nanoparticles supported by disordered mesoporous carbon: hydrogen storage performances and destabilization mechanisms. Int J Hydrogen Energy 2007;32(16):3976–80.
[93] Li HW, et al. Effects of ball milling and additives on dehydriding behaviors of well-crystallized Mg(BH4)2. Scripta Mater 2007;57(8):679–82.
[94] Li HW, et al. Dehydriding and rehydriding processes of well-crystallized Mg(BH4)2 accompanying with formation of intermediate compounds. Acta Mater 2008;56(6):1342–7.
[95] Rönnebro E, Majzoub EH. Calcium borohydride for hydrogen storage: catalysis and reversibility. J Phys Chem B 2007;111(42):12045–7.
[96] Kim J-H, et al. Reversible hydrogen storage in calcium borohydride Ca(BH4)2. Scripta Mater 2008;58(6):481–3.
[97] Chen P, et al. Interaction of hydrogen with metal nitrides and imides. Nature 2002;420(6913):302–4.
[98] Luo W. (LiNH2–MgH2): a viable hydrogen storage system. J Alloys Compd 2004;381(1):284–7.
[99] Wallace W, Karlicek R, Imamura H. Mechanism of hydrogen absorption by lanthanum-nickel (LaNi5). J Phys Chem 1979;83(13):1708–12.
[100] Joubert J-M, et al. LaNi5 related AB5 compounds: structure, properties and applications. J Alloys Compd 2021;862:158163.
[101] Kandavel M, et al. Solubility and diffusion of hydrogen in AB2-type Laves phase alloys. J Alloys Compd 2005;404–406:265–8.
[102] Wan C, Denys RV, Yartys VA. Effects of Ti substitution for Zr on the electrochemical characteristics and structure of AB2-type Laves-phase alloys as metal hydride anodes. J Alloys Compd 2021;889:161655.
[103] Zaluski L, et al. Effects of relaxation on hydrogen absorption in Fe Ti produced by ball-milling. J Alloys Compd 1995;227(1):53–7.
[104] Stampfer Jr JF, Holley Jr C, Suttle J. The magnesium-hydrogen system1-3. J Am Chem Soc 1960;82(14):3504–8.
[105] Fukai Y. The metal-hydrogen system: basic bulk properties, 21. Springer Science & Business Media; 2006.
[106] Wang L, Yang RT. Hydrogen storage on carbon-based adsorbents and storage at ambient temperature by hydrogen spillover. Catal Rev 2010;52(4):411–61.
[107] Dillon AC, et al. Storage of hydrogen in single-walled carbon nanotubes. Nature 1997;386(6623):377–9.
[108] Masika E, Mokaya R. Preparation of ultrahigh surface area porous carbons templated using zeolite 13X for enhanced hydrogen storage. Prog Nat Sci: Mater Int 2013;23(3):308–16.
[109] Gangu KK, et al. Characteristics of MOF, MWCNT and graphene containing materials for hydrogen storage: a review. J Energy Chem 2019;30:132–44.
[110] Ghosh S, Singh JK. Hydrogen adsorption in pyridine bridged porphyrin-covalent organic framework. Int J Hydrogen Energy 2019;44(3):1782–96.
[111] Lototskyy MV, Tarasov BP, Yartys VA. Gas-phase applications of metal hydrides. J Energy Storage 2023;72:108165.
[112] Xiao J, et al. An investigation into the multi-parameter identification and model optimization strategy of the PCT curves of hydrogen storage alloys by multiple intelligent algorithms. Int J Hydrogen Energy 2023;48(5):1943–55.
[113] Demirocak DE, et al. Volumetric hydrogen sorption measurements – uncertainty error analysis and the importance of thermal equilibration time. Int J Hydrogen Energy 2013;38(3):1469–77.
[114] Sheehan DP. A symmetric van 't Hoff equation and equilibrium temperature gradients. J Non-Equilibrium Thermodyn 2018;43(4):301–15.
[115] Fukumoto Y, et al. Effect of alloy composition on enthalpy and entropy changes of hydride formation for stoichiometric and nonstoichiometric hydrogen storage alloys. J Alloys Compd 1996;240(1):76–8.
[116] Hou C-p, et al. Enthalpy change (ΔH0) and entropy change (ΔS0) measurement of CeMn1−xAl1−xNi2x (x=0.00, 0.25, 0.50 and 0.75) hydrides by electrochemical P–C–T curve. Int J Hydrogen Energy 2008;33(14):3762–6.
[117] Crank J. The mathematics of diffusion. Oxford university press; 1979.
[118] Zhou G, Wong M-T, Zhou G-Q. Diffusion-controlled reactions of enzymes: an approximate analytic solution of Chou's model. Biophys Chem 1983;18(2):125–32.
[119] Jägle EA, Mittemeijer EJ. The kinetics of grain-boundary nucleated phase transformations: simulations and modelling. Acta Mater 2011;59(14):5775–86.
[120] Grosjean MH, et al. Hydrogen production via hydrolysis reaction from ball-milled Mg-based materials. Int J Hydrogen Energy 2006;31(1):109–19.
[121] Suryanarayana C. Mechanical alloying and milling. Prog Mater Sci 2001;46(1):1–184.
[122] Liang G, et al. Catalytic effect of transition metals on hydrogen sorption in nanocrystalline ball milled MgH2–Tm (Tm=Ti, V, Mn, Fe and Ni) systems. J Alloys Compd 1999;292(1):247–52.
[123] Jung KS, Lee EY, Lee KS. Catalytic effects of metal oxide on hydrogen absorption of magnesium metal hydride. J Alloys Compd 2006;421(1):179–84.
[124] Shao H, et al. Fabrication, hydrogen storage properties and mechanistic study of nanostructured Mg50Co50 body-centered cubic alloy. Scripta Mater 2009;60(9):818–21.
[125] Shao H, Felderhoff M, Schüth F. Hydrogen storage properties of nanostructured MgH2/TiH2 composite prepared by ball milling under high hydrogen pressure. Int J Hydrogen Energy 2011;36(17):10828–33.
[126] Dam B, et al. Combinatorial thin film methods for the search of new lightweight metal hydrides. Scripta Mater 2007;56(10):853–8.
[127] Qu J, et al. Hydrogen absorption kinetics of Mg thin films under mild conditions. Scripta Mater 2010;62(5):317–20.
[128] Zou J, et al. Study on the hydrogen storage properties of core–shell structured Mg–RE (RE = Nd, Gd, Er) nano-composites synthesized through arc plasma method. Int J Hydrogen Energy 2013;38(5):2337–46.
[129] Long S, et al. Hydrogen storage properties of a Mg–Ce oxide nano-composite prepared through arc plasma method. J Alloys Compd 2013;580:S167–70.

[130] Long S, et al. A comparison study of Mg–Y2O3 and Mg–Y hydrogen storage composite powders prepared through arc plasma method. J Alloys Compd 2014;615:S684–8.
[131] Zou J, et al. Hydrogen storage properties of Mg–TM–La (TM = Ti, Fe, Ni) ternary composite powders prepared through arc plasma method. Int J Hydrogen Energy 2013;38(21):8852–62.
[132] Prins R. Hydrogen spillover. Facts and fiction. Chem Rev 2012;112(5):2714–38.
[133] Roy A, Janotti A, Van de Walle CG. Effect of transition-metal additives on hydrogen desorption kinetics of MgH2. Appl Phys Lett 2013;102(3).
[134] Lu J, et al. Hydrogen storage properties of nanosized MgH2− 0.1 TiH2 prepared by ultrahigh-energy− high-pressure milling. J Am Chem Soc 2009;131(43):15843–52.
[135] Zhang J, et al. Metal hydride nanoparticles with ultrahigh structural stability and hydrogen storage activity derived from microencapsulated nanoconfinement. Adv Mater 2017;29(24):1700760.
[136] Oelerich W, Klassen T, Bormann R. Metal oxides as catalysts for improved hydrogen sorption in nanocrystalline Mg-based materials. J Alloys Compd 2001;315(1–2):237–42.
[137] Jin S-A, et al. Dehydrogenation and hydrogenation characteristics of MgH2 with transition metal fluorides. J Power Sources 2007;172(2):859–62.
[138] Zhang J, et al. Synergistic effect of Ti and F co-doping on dehydrogenation properties of MgH2 from first-principles calculations. J Alloys Compd 2012;538:205–11.
[139] Malka IE, Czujko T, Bystrzycki J. Catalytic effect of halide additives ball milled with magnesium hydride. Int J Hydrogen Energy 2010;35(4):1706–12.
[140] Malka IE, et al. A study of the ZrF4, NbF5, TaF5, and TiCl3 influences on the MgH2 sorption properties. Int J Hydrogen Energy 2011;36(20):12909–17.
[141] Konarova M, et al. Porous MgH2/C composite with fast hydrogen storage kinetics. Int J Hydrogen Energy 2012;37(10):8370–8.
[142] Liu G, et al. Excellent catalytic effects of highly crumpled graphene nanosheets on hydrogenation/dehydrogenation of magnesium hydride. Nanoscale 2013;5(3):1074–81.
[143] Verón M, Troiani H, Gennari F. Synergetic effect of Co and carbon nanotubes on MgH_2 sorption properties. 2011.
[144] Reilly Jr JJ, Wiswall Jr RH. Reaction of hydrogen with alloys of magnesium and nickel and the formation of Mg2NiH4. Inorganic chemistry 1968;7(11):2254–6.
[145] Shao H, et al. Thermodynamic property study of nanostructured mg-H, mg-Ni-H, and mg-cu-H systems by high pressure DSC method. J Nanomater 2013:2013.
[146] Liu Y, et al. Study on hydrogen storage properties of Mg–X (X= Fe, Co, V) nanocomposites co-precipitated from solution. RSC advances 2015;5(10):7687–96.
[147] Reilly Jr JJ, Wiswall Jr RH. Reaction of hydrogen with alloys of magnesium and copper. Inorganic chemistry 1967;6(12):2220–3.
[148] Khan D, et al. Formation and hydrogen storage behavior of nanostructured Mg2FeH6 in a compressed 2MgH2–Fe composite. Int J Hydrogen Energy 2020;45(41):21676–86.
[149] Ouyang LZ, et al. A new type of Mg-based metal hydride with promising hydrogen storage properties. Int J Hydrogen Energy 2007;32(16):3929–35.
[150] Darriet B, et al. Application of magnesium rich rare-earth alloys to hydrogen storage. Int J Hydrogen Energy 1980;5(2):173–8.
[151] Dutta K, Srivastava O. Investigation on synthesis, characterization and hydrogenation behaviour of the La2Mg17 intermetallic. Int J Hydrogen Energy 1990;15(5):341–4.
[152] Ouyang L, Qin F, Zhu M. The hydrogen storage behavior of Mg3La and Mg3LaNi0.1. Scripta Mater 2006;55(12):1075–8.
[153] Zhang XL, et al. Empowering hydrogen storage performance of MgH2 by nanoengineering and nanocatalysis. Materials Today Nano 2020;9:100064.
[154] Chen Z, et al. Porous materials for hydrogen storage. Chem 2022;8(3):693–716.
[155] Ham B, et al. Size and stress dependent hydrogen desorption in metastable Mg hydride films. Int J Hydrogen Energy 2014;39(6):2597–607.
[156] Xin G, et al. Promising gaseous and electrochemical hydrogen storage properties of porous Mg–Pd films under mild conditions. Phys Chem Chem Phys 2015;17(20):13606–12.
[157] Zhou W, Wu H, Yildirim T. Enhanced H2 adsorption in isostructural Metal−Organic frameworks with open metal sites: strong dependence of the binding strength on metal ions. J Am Chem Soc 2008;130(46):15268–9.
[158] Kapelewski MT, et al. M2(m-dobdc) (M = Mg, Mn, Fe, Co, Ni) metal–organic frameworks exhibiting increased charge density and enhanced H2 binding at the open metal sites. J Am Chem Soc 2014;136(34):12119–29.
[159] Nayak NY, et al. Zeolite catalyzed friedel-crafts reactions: a review. Lett Org Chem 2020;17(7):491–506.
[160] Langmi HW, et al. Hydrogen adsorption in zeolites A, X, Y and RHO. J Alloys Compd 2003;356–357:710–5.
[161] Leick N, et al. Al2O3 atomic layer deposition on nanostructured γ-Mg(BH4)2 for H2 storage. ACS Appl Energy Mater 2021;4(2):1150–62.
[162] Schneemann A, et al. Nanoconfinement of molecular magnesium borohydride captured in a bipyridine-functionalized metal–organic framework. ACS Nano 2020;14(8):10294–304.
[163] Ma Z, et al. In situ catalyzed and nanoconfined magnesium hydride nanocrystals in a Ni-MOF scaffold for hydrogen storage. Sustain Energy Fuels 2020;4(9):4694–703.
[164] Han DJ, et al. Tailoring hierarchical pore structures in carbon scaffolds for hydrogen storage of nanoconfined magnesium. Chem Eng J 2024;481:148451.
[165] Jiang G, He G. A new approach to the fabrication of porous magnesium with well-controlled 3D pore structure for orthopedic applications. Mater Sci Eng C 2014;43:317–20.
[166] Guo N, Leu MC, Koylu UO. Bio-inspired flow field designs for polymer electrolyte membrane fuel cells. Int J Hydrogen Energy 2014;39(36):21185–95.
[167] Ding X, et al. A novel method towards improving the hydrogen storage properties of hypoeutectic Mg-Ni alloy via ultrasonic treatment. J Magnesium Alloys 2023;11(3):903–15.